Computers and Geotechnics 37 (2010) 1023–1029

Contents lists available at ScienceDirect

Computers and Geotechnics

journal homepage: www.elsevier.com/locate/compgeo

Technical Communication

Numerical solution of active earth pressures on rigid retaining walls built near rock faces

Chia-Cheng Fan [a,*], Yung-Show Fang [b,1]

[a] Dept. of Construction Engineering, National Kaohsiung First University of Science and Technology, Taiwan, ROC
[b] Dept. of Civil Engineering, National Chiao Tung University, Taiwan, ROC

ARTICLE INFO

Article history:
Received 11 March 2010
Received in revised form 6 August 2010
Accepted 6 August 2010

Keywords:
Active earth pressure
Limited backfill space
Finite element analysis
Aspect ratio

ABSTRACT

For retaining walls built in mountainous regions, narrow backfill spaces are often encountered. The space to fully develop the active wedge is restricted for walls with a limited backfill space. This paper presents a numerical study on the behaviour of active earth pressures behind a rigid retaining wall with limited backfill space of various geometries. The active earth pressure for a wall built with limited backfill space is considerably less than that of the Coulomb solution, and the location of the resultant of active earth pressures is noticeably higher than one-third of the wall height. The coefficient of active earth pressures is as low as 0.5–0.6 times the Coulomb solution and the h/H value reaches up to 0.4–0.37 if aspect ratio of the fill space is in the range from 0.1 to 0.2. A clear trend between the ratio of the coefficient of active earth pressures at constrained fill conditions over the Coulomb K_a value and the aspect ratio of the fill-space geometry is obtained.

1. Introduction

The Coulomb or Rankine theories are commonly used for computing active earth pressures behind rigid retaining walls in wall design. Both of the theories require that the backfill behind the wall extend to a sufficient distance and that the failure wedge develop fully in the backfill. However, for walls built in mountainous regions, e.g., the case reported by Fan and Hsieh [4] and Lee and Hencher [9], narrow backfill widths are often encountered, e.g., rock formations or stable boundaries are close to the wall, as shown in Fig. 1. For rigid retaining walls, the active failure wedge in the backfill is bounded by the wall and the plane with an inclination angle of $(45° + \phi/2)$ from the horizontal, as shown in Fig. 1. Any stiff boundary, e.g., stable rock faces, within the failure wedge may result in interference of the development of the active state behind the wall. For rigid retaining walls built adjacent to rock faces, the commonly used Coulomb and Rankine theories are clearly inappropriate in estimating the active earth pressure on the wall. The distribution of earth pressures on retaining walls with limited backfill space has gained little attention in past research, whereas it is important in the design of reinforced concrete (RC) retaining walls in mountainous regions in terms of the resultant of earth pressures and the location of the resultant of earth pressures.

Frydman and Keissar [6] conducted centrifuge model tests for a rigid retaining wall near a vertical rigid boundary to observe changes in earth pressures behind the wall from at-rest conditions to active conditions. The retaining wall was made from aluminium, allowing rotation of the wall about its base. The test results showed that the earth pressure in active conditions was not in a triangular distribution. The coefficient of active earth pressures, defined as the ratio of the horizontal stress over the overburden stress, decreased noticeably with the depth. In other words, the location of the resultant of active earth pressures was located above one-third of the wall height.

Spangler and Handy [12] developed an equation based on Janssen's arching theory [8] for calculating the lateral pressure acting on the wall of a silo. The lateral pressure at any given depth, z, is given as (silo pressure equation)

$$\sigma_h = \frac{\gamma b}{2\tan\delta}\left[1 - \exp\left(-2K\frac{z}{b}\tan\delta\right)\right] \quad (1)$$

where σ_h is the lateral pressure acting on the wall, b is the distance between the walls, K is the coefficient of lateral pressure on the wall, z is the depth from the top of the wall, γ is the unit weight of the filled material, and δ is the angle of friction between the wall and the fill. The K value depends on the movement of the wall. For walls without movement, Jaky's equation was suggested for estimating the K value, i.e., $K = 1 - \sin\phi$ [6]. In the active condition, Frydman and Keissar [6] further derived the K value by taking into

* Corresponding author. Address: 2, Jhuoyue Rd., Nanzih District, Kaohsiung City, Taiwan 811, ROC. Tel.: +886 7 6011000x2117; fax: +886 7 6011017.
E-mail address: ccfan@ccms.nkfust.edu.tw (C.-C. Fan).
[1] Address: 1001 Ta Hsueh Road, Hsinchu, Taiwan 30010, ROC. Tel.: +886 3 572 5634; fax: +886 3 572 8504.

0266-352X/$ - see front matter © 2010 Elsevier Ltd. All rights reserved.
doi:10.1016/j.compgeo.2010.08.004

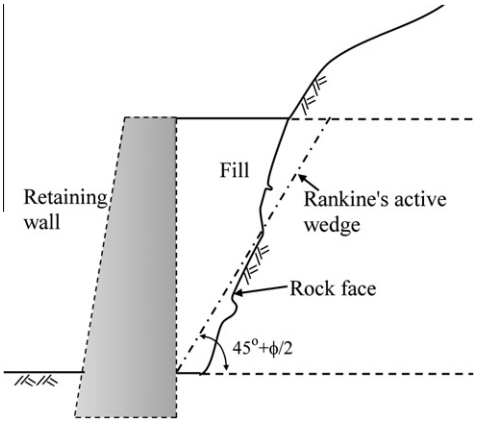

Fig. 1. A schematic drawing of a RC retaining wall near a rock face.

account the friction between the wall and the fill and assuming that the soil near the wall reached a state of failure. The K value is given by

$$K=\frac{(\sin^2\phi+1)-\sqrt{(\sin^2\phi+1)^2-(1-\sin^2\phi)(4\tan^2\delta-\sin^2\phi+1)}}{(4\tan^2\delta-\sin^2\phi+1)} \tag{2}$$

where ϕ is the angle of internal friction of the fill. The coefficient of lateral earth pressures in the active condition at a given depth z can be determined as the ratio of σ_h over σ_v ($=\gamma z$) and is expressed as

$$K_a=\frac{b}{2(z)\tan\delta}\left[1-\exp\left(-2K\frac{z}{b}\tan\delta\right)\right] \tag{3}$$

The coefficient of active earth pressures at a given depth z for retaining walls near vertical rock faces can be theoretically estimated by substituting Eq. (2) into Eq. (3). The distribution of the K_a value with the depth in Eq. (3) was verified using the experimental data obtained from the centrifuge model tests [6], in which the model wall rotated about its base. The K_a value obtained decreased considerably with depth. Additionally, the measured K_a value was significantly less than the Coulomb's coefficient of active earth pressures at a z/b value greater than about 2.0. The measured K_a value was in a range from 0.22 to 0.25 at a z/b value of 2, whereas it was about 0.14 at a z/b value of 6.5. The Coulomb K_a value for the soil ($\phi = 36°$ and $\delta = 25°$) used in the centrifuge model test was 0.235. Nevertheless, the equations shown above cannot be used to compute the active earth pressure on traditional rigid retaining walls with limited backfill space because the geometry of the backfill space is unlike that of a silo.

Although experimental studies are rare, the behaviour of active earth pressures against rigid retaining walls near a vertical stiff boundary has been identified experimentally by Frydman and Keissar [6]. However, little attention has been paid to the location of the resultant of active earth pressures and the active earth pressure on rigid retaining walls built next to constrained fill space with various geometric conditions. The research conducted herein aims to investigate this subject. The finite element method was used to carry out the analyses. Additionally, the effect of the wall height and the friction angle of the backfill soil on the active earth pressure as well as the location of the resultant of active earth pressures for walls with limited backfill space were also investigated in this study.

2. Numerical modelling

2.1. Finite element modelling

The non-linear finite element program PLAXIS [10] was used to analyse the earth pressure from at-rest to active conditions for a rigid retaining wall close to a stable rock face. Typical geometry of the backfill zone used in this study is shown in Fig. 2. The wall used in the analyses represents a rigid RC wall, i.e., no bending during wall movement, in the FE model. To investigate the influence of the backfill-space geometry on the behaviour of active earth pressures, the sloping gradient (β) of the rock face and the distance (b) between the bottom of the wall and the rock face were varied in the numerical analyses. The soil at the base of the wall was considered a firm ground in the numerical analyses conducted herein. The numerical analyses on earth pressures reaching active states on a wall were conducted by using displacement-controlled numerical scheme on the wall movement. The bottom boundary of the mesh was fixed against movement in horizontal and vertical directions, and the vertical boundaries of the mesh were fixed against horizontal movement.

The wall was prevented from movement during placing the fill. Wall movement was prescribed after the filling process until earth pressures behind the wall reach the active condition. The finite element mesh, which was examined to eliminate the influence of size effect and boundary on the results of the analyses, for a retaining wall with limited backfill space ($\beta = 70°$ and $b = 0.5$ m) is shown in Fig. 3. The finite element mesh consisted of 1512 elements, 3580 nodes, and 4536 stress points.

2.2. Modelling of backfill, walls, and interfaces

Soil elements used in this study were six-node triangular isoparametric elements, with three Gauss points for each element. The Mohr–Coulomb constitutive model was used to model the stress–strain behaviour of soils. This model requires five parameters, i.e., Young's modulus (E), Poisson's ratio (ν), friction angle (ϕ), cohesion (c), and dilatancy angle (ψ). The dilatancy angle (ψ) is normally used in cohesionless materials and is dependent on the relative density and friction angle of the soil. For a soil material with friction angle greater than 30°, the soil tends to dilate at small strain conditions, where active earth pressures develop. The dilatancy angle (ψ) is approximately equal to $\phi - 30°$ [2], and it is used in the current study.

Interface elements between the wall and the backfill and between the rock face and the backfill were taken into account in the analyses. Thin rectangular interface elements, six-node elements, were used between soils and structural elements [10]. The interface element had a zero thickness in the finite element formulation. However, a small virtual thickness was assigned to the interface element, which was used to define the material prop-

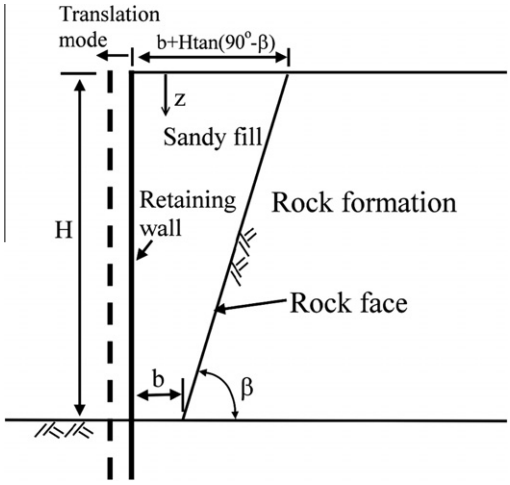

Fig. 2. Typical geometry of backfill zone behind a retaining wall and the type of wall movement (translation mode) used in this study.

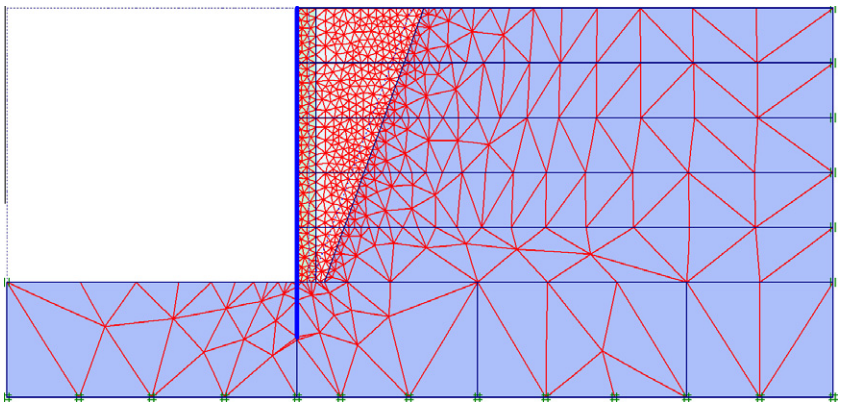

Fig. 3. The finite element mesh for a retaining wall with limited backfill space ($\beta = 70^\circ$ and $b = 0.5$ m).

erties of the interface. The material properties of the interface element were the same as those of surrounding soil elements, except that a strength reduction factor (R_{inter}), defined as the ratio of the interface strength to the shear strength of surrounding soils, was used for the interface element. Contact modes, slip modes, and de-bonding modes were considered in the interface element. The experimental results conducted by Ampera and Aydogmus [1] indicated that the interface friction angle (δ) between silty materials and smooth concrete ranged from about 0.74ϕ to 0.9ϕ, and the δ value between silty materials and rough concrete ranged from 0.98ϕ to 1.02ϕ. Additionally, Potyondy [11] proposed that the δ/ϕ values between sands and concrete made in wood form and those between sands and rough concrete were 0.88 and 0.98, respectively, in dry condition. Therefore, δ/ϕ value of 0.9 was used for the interface friction angle (δ_1) between the backfill and the wall in this study, and a δ/ϕ value of 1.0 was used for the interface friction angle (δ_2) between the backfill and the rock face.

The rock formation behind the retaining wall was considered a stable ground. The stress–strain behaviour of the rock formation was considered to have no influence on the stress distribution in the backfill soil during filling. Linear elastic behaviour was used to model the behaviour of the rock formation. Additionally, the retaining wall used in the analyses was a rigid reinforced concrete structure with a uniform thickness of 0.6 m. It was modelled using plates with linearly elastic behaviour in the FE analysis. The analyses were conducted in dry conditions.

2.3. Verifications

Earth pressures computed from the FE analyses for walls undergoing lateral movement were verified using the experimental data obtained from centrifuge model wall tests conducted by Frydman and Keissar [6] and the Spangler and Handy equation, Eq. (3), associated with Eq. (2). The retaining wall in the centrifuge model test was close to a vertical rock face, which was simulated by wooden block coated with sands. Fine sand was used for the backfill. The wall was prevented from movement during the filling with sands. Walls allowed for rotation about their base after the filling. The sand was prepared at a relative density of 70% in the model tests, and the friction angle (ϕ) of the fill in the model tests was 36°. The interface friction angle between the wall (aluminium) and the sand was 20–25°, and a friction angle of 25° was used for the interface between the wall and the backfill in the FE analyses. The interface friction angle between the backfill and the rock face was 30°; the unit weight of the sand was 15.8 kN/m^3 [6]. The centrifuge model wall test corresponded to a wall height of 8.5 m. The FE analyses were conducted for an 8.5-m-high wall. The fill in the FE modelling was completed in eight stages, 1-m-thick per stage from the bottom to a height of 7 m and 1.5 m thick for the last stage. The fill was placed as an elastic material and converted to a material with the Mohr–Coulomb soil model the next stage. The FE mesh was similar to that shown in Fig. 3, whereas the bottom of the wall was located at the same elevation as that of ground surface in front of the wall. Following the completion of the filling, lateral displacements were prescribed on the wall to allow rotation about its bottom until active conditions were reached. The FE analyses for fill widths (b) of 1 m and 2 m were carried out. Fig. 4 shows the comparison among the computed active earth pressures from the FE analyses, the theoretic solution, and the measured data from the centrifuge model wall test. Good agreement was obtained among these results.

3. Active earth pressures on retaining walls with limited backfill space

Typical geometry of the backfill zone behind retaining walls considered in this study is shown in Fig. 2. The wall height (H) used

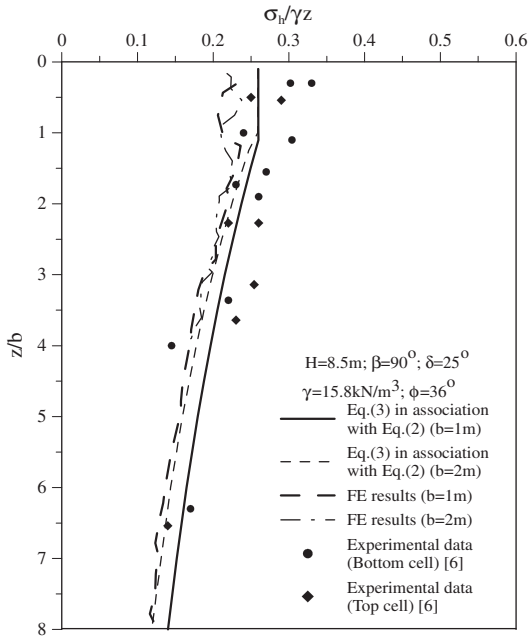

Fig. 4. Comparison of the distribution of active earth pressures along depth (z/b) among the FE results, experimental data, and theoretical solution (*Note*: the top and bottom cells in the experimental study [6] were located at the 2/3 and 1/3 of the wall height, respectively).

was 5 m, and the embedment depth of the wall was 1 m. The fill width (b) at the bottom of the wall and inclination (β) of the rock face were varied in the FE analyses. The fill widths (b) were 0 m, 0.5 m (0.1H), and 1 m (0.2H), and the inclinations (β) of the stiff boundary (rock faces) varied from 30° to 90°. The retaining wall was considered to be undergoing translation in this study. The schematic drawing for this type of wall movement is shown in Fig. 2. Walls were prevented from moving during placement of the backfill, and wall movements were prescribed in the FE analyses following the completion of backfilling until earth pressures reached the active condition.

Table 1 shows the parameters used for the wall, the backfill soil, and the rock formation in the FE analyses. The parameters for the backfill soil are typical for medium to dense sandy materials.

3.1. Distribution of earth pressures along depth

For rigid retaining walls with a height of 5 m and a friction angle of 31° for the backfill, the Rankine's active failure wedge intersects with the top surface at a distance of 2.83 m from the wall. Computing the active earth pressure using the Coulomb earth pressure theory is inappropriate if the active failure wedge cannot fully develop due to the geometric constraints of the rock face. Fig. 5 shows the horizontal earth pressure distribution with depth (z/H) at various wall displacements at a β value of 80° and a b value of 0.5 m. The horizontal earth pressures were obtained through the normal stresses of a vertical cross-section in the backfill right behind the wall. The earth pressure in active conditions occurs at a wall displacement of about 0.0005H. The earth pressure in active conditions along the depth is not in a triangular distribution, and it is considerably less than that of the Coulomb solution at the lower elevation of the wall. The resultant of active earth pressures is obviously less than that computed using the Coulomb theory, and the location of the resultant of the active earth pressure is about 0.38H (>1/3H).

Fang and Ishibashi [5] carried out model wall tests for earth pressures under different modes of wall movement, i.e., rotation about the wall base, rotation about the wall top, and translation. The authors reported that the wall displacement at its top required to reach active earth pressure conditions behind the wall was about 0.0005H for a wall moving in translation mode. Bowles [3] indicated that the amount of translation required to produce active earth pressure conditions was about 0.001H–0.002H and 0.002H–0.004H for dense and loose cohesionless materials, respectively. The wall movement required to reach the active state obtained in the numerical analyses was less than that proposed by Bowles [3]; however, it was similar to that obtained in the model wall test carried out by Fang and Ishibashi [5].

In addition, the coefficient of active earth pressures ($K_{a(c)}$) computed from the FE analyses is defined as

$$K_{a(c)} = \frac{P_A}{0.5\gamma H^2(\cos\delta)} \tag{4}$$

where P_A is the resultant of horizontal earth pressures in active conditions computed from the FE analyses, γ is the unit weight of backfill, H is the wall height, and δ is the friction angle of the wall-soil interface. For the backfill space with a b value of 0.5 m and a β value of 80°, the $K_{a(c)}$ value is 0.234, which is less than the Coulomb solution ($K_{a(Coulomb)}$ = 0.286). Furthermore, the $K_{a(c)}$ value is 0.30 if the backfill space is sufficient (e.g., b = 10 m) to develop active wedge in the numerical modelling used herein, and the $K_{a(c)}$ value is about 1.05 times the $K_{a(Coulomb)}$ value.

The behaviour of active earth pressures obtained for walls with limited backfill space can be attributed to the arching effect developed in the backfill. It is induced by the cumulative effect of side friction forces along the side boundaries of the backfill during filling [7]. The cumulative side forces along the wall work to reduce the total vertical force near the wall as a function of depth. Fig. 6 shows the principal stress distributions in the backfill for walls undergoing translation in active conditions at a b value of 0.5 m and a β value of 80°. The principal stress directions in the backfill vary with depth due to the confined effect of the rock face behind the wall and the side friction developed between the backfill and the wall. The trajectory of the minor principal stress direction in the backfill shows an approximately continuous arch that dips downward, i.e., an inverted arch, and the minor principal stress trajectory forms about a half-arch at about the mid-height to one-fifth of the wall height due to the presence of an inclined rock face. Additionally, small lateral stresses at the lower elevation of the backfill near the wall were observed. The numerical results further prove the theoretical work on soil arching introduced by Handy [7]: soil arching action may be depicted as a trajectory of the minor principal stress that approximates a catenary.

Table 1
Parameters for the backfill, the rock, and walls used in the FE analyses.

Parameters	Backfill (Mohr–Coulomb model)	Rock (linearly elastic)	Wall (linearly elastic)
Unit weight (γ_t)	15.5 kN/m^3	24 kN/m^3	24 kN/m^3
Cohesion (c)	0	–	–
Friction angle (ϕ)	31°	–	–
Modulus of elasticity (E)	60 MPa	2100 MPa	2100 MPa
Poisson's ratio (ν_{ur})	0.3	0.15	0.15
Dilatancy angle (ψ)	1°	–	–
Interface friction angle between the wall and the backfill(δ_1)	28°	–	–
Interfac e friction angle between the rock face and the backfill (δ_2)	31°	–	–
Flexural rigidity (EI)	–	–	4.2×10^5 kN m^2/m
Normal stiffness (EA)	–	–	1.26×10^7 kN/m

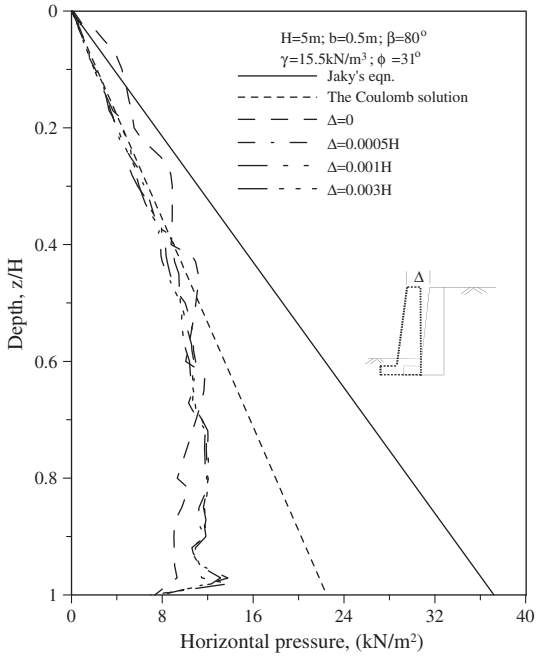

Fig. 5. Distribution of horizontal earth pressures with the depth at various wall displacements.

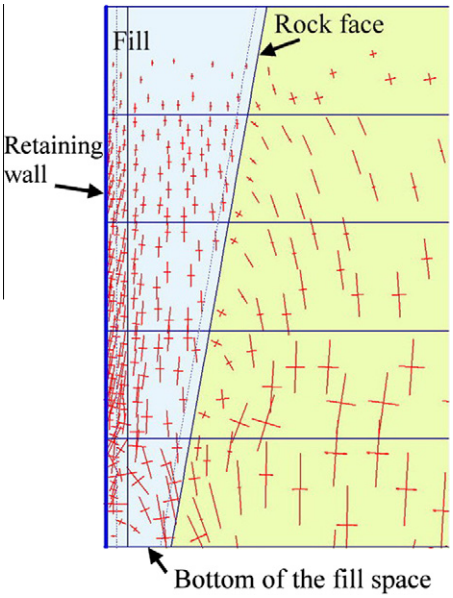

Fig. 6. The principal stresses in the backfill ($\beta = 80°$, $b = 0.5$ m) behind a wall in active conditions.

3.2. Effect of fill-space geometry on active earth pressures

The location of the rock face behind retaining walls plays an important role in the development of arching in the backfill and in the mobilisation of earth pressures on the wall. Fig. 7 shows the variation of the ratio of the coefficient of active earth pressures, $K_{a(c)}$, computed from FE analyses over the Coulomb solution, $K_{a(Coulomb)}$, with the inclination (β) of the rock face at various fill widths (b). The $K_{a(c)}$ values for β greater than about 60° are considerably less than those of the Coulomb solution and decrease with increasing β values. Additionally, the $K_{a(c)}$ values decrease with decreasing fill width (b) at a given β value greater than about 60°. For the rock face with β values of 90°, 80°, and 70°, the $K_{a(c)}$ values are 0.51, 0.82, and 1.02 times the Coulomb K_a value (=0.286) if the fill width (b) is 0.5 m. The influence of the rock face on the development of earth pressures in the backfill can be neglected if the β value is less than about 60°, which is close to the inclination of the active wedge ($=45° + \phi/2 = 60.5°$). For b values of 0 m, 0.5 m, and 1 m, the $K_{a(c)}$ values are 0.60, 0.82, and 0.95 times the Coulomb K_a value if the β value is 80°.

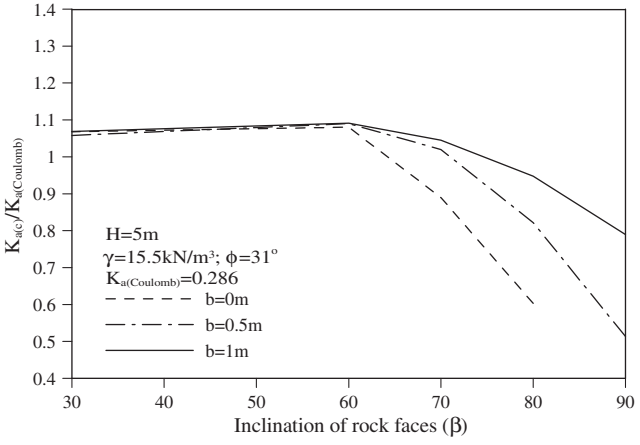

Fig. 7. Variation of the coefficient of active earth pressures ($K_{a(c)}/K_{a(Coulomb)}$) with the inclination of rock faces at various fill widths (b).

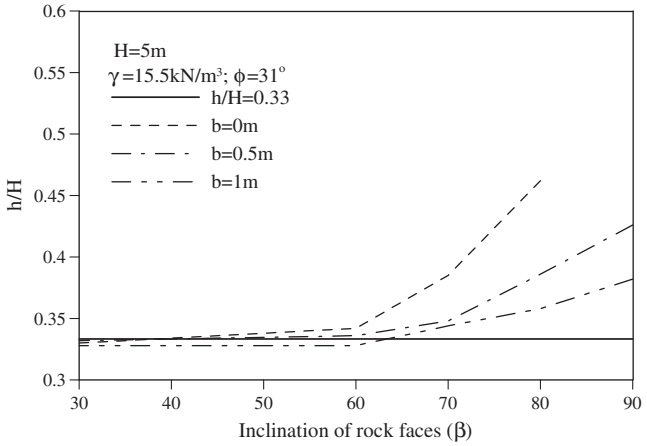

Fig. 8. Variation of the location of the resultant (h/H) of active earth pressures with the inclination of rock faces at various fill widths (b).

3.3. Effect of fill-space geometry on the location of the resultant of active earth pressures

Fig. 8 shows the variation of the location (h/H), measured from the ground surface in front of the wall, of the resultant of active earth pressures with the inclination (β) of rock faces at various fill widths (b). The locations of the resultant of active earth pressures are greater than $0.33H$, which is the location of the resultant for a triangular earth pressure distribution, for fill space with a β value greater than about 60°, and they are almost the same as $0.33H$ at a β value less than about 60°. For a β value greater than 60°, the h/H value increases with increasing β values, and it increases with decreasing fill widths. For walls with b value of 0.5 m, the h/H values reach up to 0.42, 0.39 and 0.35 for the rock face inclined at 90°, 80°, and 70°, respectively.

4. Effect of aspect ratio of the fill space on active earth pressures

The coefficient of lateral earth pressures in the active condition at a given depth (z) for retaining walls near a vertical stiff boundary is a function of the fill width (b) and depth (z) according to the theoretic derivation by Frydman and Keissar [6], as shown in Eq. (3). Thus, wall height may affect the coefficient of active earth pressures for walls close to rock faces. Numerical analyses on retaining walls 3 m, 5 m, and 8 m high were further carried out in this study. To demonstrate the effect of the geometry of the limited backfill space on the active earth pressure, the ratio of the fill width at the top of the backfill, $b + H \cdot \tan(90° - \beta)$, over the wall height ($H$) was defined to represent the aspect ratio of the fill space. Figs. 9 and 10 show the variations of the $K_{a(c)}/K_{a(Coulomb)}$ value and the h/H value with the ratio of $(b + H \cdot \tan(90° - \beta))/H$, respectively. A clear trend between the $K_{a(c)}/K_{a(Coulomb)}$ value and the aspect ratio, $(b + H \cdot \tan(90° - \beta))/H$, was observed. Additionally, the relationship between the h/H value and the aspect ratio was also clearly identified. The $K_{a(c)}/K_{a(Coulomb)}$ value decreases with decreasing aspect ratio, $(b + H \cdot \tan(90° - \beta))/H$. The $K_{a(c)}/K_{a(Coulomb)}$ values level off once the aspect ratio is greater than about 0.6, and the $K_{a(c)}$ value is slightly greater than the Coulomb solution at a high aspect ratio. The h/H value increases with decreasing aspect ratio of the fill space and reaches 0.33 at an aspect ratio greater than about 0.6.

In addition, the effect of the friction angle (ϕ) of the backfill soil on the relationship between the normalised coefficient of active earth pressures ($K_{a(c)}/K_{a(Coulomb)}$) and the aspect ratio of the fill space was further analysed, as shown in Fig. 11. Friction angles of 25°, 31°, and 35°, which cover the soil properties for most of

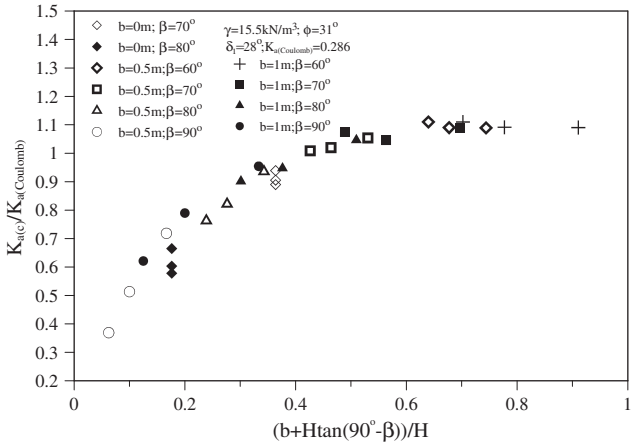

Fig. 9. Variation of $K_{a(c)}/K_{a(Coulomb)}$ with aspect ratio of the fill space $((b + H\tan(90^\circ - \beta))/H)$.

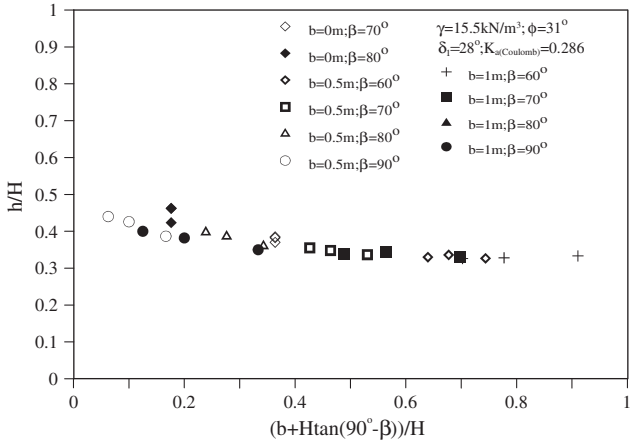

Fig. 10. Variation of the location of the resultant of active earth pressures (h/H) with aspect ratio of the fill space $((b + H\tan(90^\circ - \beta))/H)$.

the fill materials, were used in the analyses. The trend found by the authors is a very good approximation for the full range of friction angle. The equation and accuracy for estimating the $K_{a(c)}/K_{a(Coulomb)}$ value with respect to the aspect ratio is shown Fig. 11. Fig. 12 shows the variation of the h/H value with aspect ratio of the fill space for various friction angles. These results demonstrate that

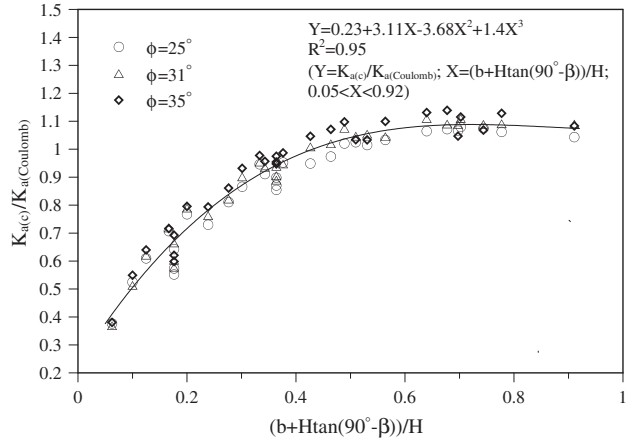

Fig. 11. Influence of friction angle of the soil on the variation of $K_{a(c)}/K_{a(Coulomb)}$ with aspect ratio of the fill space.

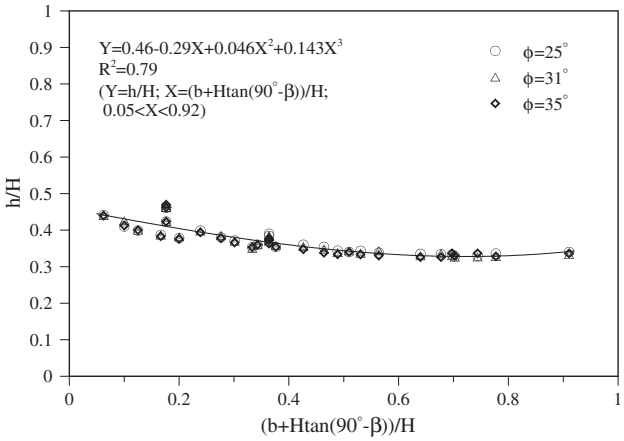

Fig. 12. Influence of friction angle of the soil on the variation of h/H with aspect ratio of the fill space.

the effect of friction angle of the soil on the correlations between the $K_{a(c)}/K_{a(Coulomb)}$ and the aspect ratio and between the h/H and the aspect ratio is negligible. The equation for estimating the h/H value with respect to the aspect ratio is summarised in Fig. 12.

5. Conclusions

This paper investigated active earth pressures on rigid retaining walls built near rock faces. The fill space behind the wall was limited due to the presence of the rock face. The finite element method was used to carry out the analyses. Rock faces behind the fill space with various sloping conditions and with various distances from the wall were taken into account in the FE analyses. In addition, the effect of the aspect ratio of the fill space and the friction angle of the fill on the coefficient of active earth pressures and the location of the resultant of active earth pressures was also investigated in this study.

The coefficients ($K_{a(c)}$) of the active earth pressures on rigid walls near rock faces were considerably less than the Coulomb solution and decreased with increasing inclination (β) of the rock face if the stiff boundary was within the Rankine's active wedge. For rock faces with β angle of 80°, the $K_{a(c)}$ value was 0.60, 0.82, and 0.95 times the Coulomb K_a value at the fill width (b) of 0, 0.5 m, and 1 m, respectively, at the bottom. The presence of the rock face within the active wedge resulted in a higher location of resultant of active earth pressures, i.e., $h/H > 0.33$. The h/H value increased with increasing inclinations (β) of the rock face, and it increased with decreasing fill widths (b). For rock faces with a β angle of 80°, the h/H values reached up to 0.46, 0.39 and 0.36 at the fill width (b) of 0 m, 0.5 m, and 1 m, respectively, at the bottom. Additionally, a simple relationship between the normalised coefficient ($K_{a(c)}/K_{a(Coulomb)}$) of active earth pressures on walls near rock faces and the aspect ratio of the fill space was obtained irrespective of the wall height and the friction angle of the fill materials. The $K_{a(c)}/K_{a(Coulomb)}$ value decreased with the decreasing aspect ratio of the fill space, and it levelled off at an aspect ratio of about 0.6. Additionally, a clear relationship between the h/H value and the aspect ratio of the fill space was also obtained irrespective of the wall height and the friction angle of the fill materials. The h/H value increased with the decreasing aspect ratio of the fill space.

Acknowledgements

The authors thank Mr. Kuang-Hui Chen and Mr. Jiun-Hung Luo, who helped conduct some of the analyses.

References

[1] Ampera B, Aydogmus T. Skin friction between peat and silt soils with construction materials. Electronic Journal of Geotechnical Engineering 2005;10(D):13p.
[2] Bolton MD. The strength and dilatancy of sands. Geotechnique 1986;36(1):65–78.
[3] Bowles JE. Foundation analysis and design. McGraw-Hill Companies Inc.; 1996.
[4] Fan CC, Hsieh CC. A hybrid reinforced embankment system used in mountainous roadways. In: 16th Southeast Asia geotechnical conference, Kuala Lumpur, Malaysia; 2007.
[5] Fang YS, Ishibashi I. Static earth pressure pressures with various wall movements. Journal of Geotechnical Engineering ASCE 1986;112(3):317–33.
[6] Frydman S, Keissar I. Earth pressure on retaining walls near rock faces. Journal of Geotechnical Engineering ASCE 1987;113(6):586–99.
[7] Handy R. The arch in soil arching. Journal of Geotechnical Engineering ASCE 1985;111(3):302–18.
[8] Janssen HA. Versuche uber Getreidedruck in Silozellen. Z Ver Deut Ingr 1895;39:1045–49 (partial English translation in proceedings of institute of civil engineers, London, England; 1896. p. 553)
[9] Lee SG, Hencher SR. The repeated failure of a cut-slope despite continuous reassessment and remedial works. Engineering Geology 2009;107:16–41.
[10] PLAXIS BV. User's manual of PLAXIS, A.A. Balkema Publishers; 2002.
[11] Potyondy JG. Skin friction between various soils and construction materials. Geotechnique 1961;11(4):339–53.
[12] Spangler MG, Handy RL. Soil engineering. New York: Harper and Row; 1984.